scientific reports

Check for updates

OPEN

Immunomodulatory vaccine demonstrates therapeutic efficacy across cancer types

Tiyun Han[3,5], Guilai Liu[3,5], Chenyi Bao[1,4,5], Jian Zong[2], Caiyi Fei[3], Jing Li[3], Shi Xu[3]✉, Qingbo Ma[2]✉ & Yingjuan Qian[1,4]✉

Immunosuppression within the tumor microenvironment (TME) profoundly inhibits anti-tumor immunity, presenting a formidable challenge in cancer therapeutics. Despite this recognized obstacle, multi-targeted immunomodulatory strategies remain elusive. Here we developed a novel mRNA-lipid nanoparticle (LNP) vaccine designed to reprogram key cellular mediators of immune suppression within the TME, including C-C motif chemokine ligand 22 (CCL22), transforming growth factor-β (TGF-β), cytotoxic T-lymphocyte-associated protein 4 (CTLA-4), Galectin-3, programmed cell death ligand 1 (PD-L1), indoleamine 2,3-dioxygenase 1 (IDO1), and arginase 1 (ARG1). This immunomodulatory vaccine was evaluated in a cohort of canines with spontaneous neoplasms, encompassing adrenal, hepatic, perianal, vulvar, and pulmonary malignancies. The vaccine demonstrated good tolerability, with only mild adverse events (Grade 1 anorexia, chills, and fatigue) observed in 25% of subjects (2/8). Remarkably, 75% of treated animals (6/8) achieved stable disease, with the median progression-free interval not yet reached a median follow-up of 168 days post-treatment initiation. Two dogs experienced disease progression. The overall disease control rate was 75%. In addition, vaccine administration reversed hematological and biochemical abnormalities and alleviated paraneoplastic syndromes associated with these malignancies. These findings demonstrate that our mRNA-LNP vaccine effectively exerts anti-tumor effects across various cancer types, offering a promising strategy for enhancing anti-tumor immunity in both veterinary and human oncology.

Keywords mRNA-LNP, Immunomodulatory vaccine, Tumor microenvironment, Canine cancer, Multi-targeted

The advent of cancer immunotherapy has transformed current approaches to treating malignancies, yet the full potential of these therapies remains constrained by the immunosuppressive tumor microenvironment (TME). Despite significant advances, many patients fail to respond to current immunotherapeutic strategies, highlighting the urgent need for novel approaches to overcome TME-mediated immune evasion[1–4]. The TME orchestrates a sophisticated network of immunosuppressive mechanisms, effectively shielding tumors from immune surveillance and attenuating the potency of anti-tumor immune responses. Key cellular mediators of this immunosuppression include regulatory T cells (Tregs), myeloid-derived suppressor cells (MDSCs), cancer-associated fibroblasts (CAF)and tumor-associated macrophages (TAMs)[5–8]. These cells employ diverse mechanisms to inhibit effector T cell function, promote angiogenesis, and facilitate tumor escape from immune surveillance. The critical role of the TME in modulating treatment outcomes has spurred intense research into strategies that can effectively reprogram this immunosuppressive milieu, with the ultimate goal of enhancing the efficacy of existing immunotherapies and developing novel therapeutic approaches.

In recent years, considerable effort has been devoted to developing immunomodulatory vaccines targeting specific components of the TME. Single-target approaches have shown promise in preclinical and early clinical studies. Vaccines targeting Tregs have demonstrated the ability to deplete or functionally modulate these suppressive cells, leading to enhanced anti-tumor immunity in some cancer models[9,10]. Similarly, vaccines reprogramming TAMs from a pro-tumoral M2-like phenotype to an anti-tumoral M1-like phenotype have

[1]MOE Joint International Research Laboratory of Animal Health and Food Safety, College of Veterinary Medicine, Nanjing Agricultural University, Nanjing 210095, Jiangsu Province, China. [2]Ai-Bi Pet Hospital, Nanjing 210049, Jiangsu Province, China. [3]Nanjing Chengshi (TheraRNA) Biomedical Technology Co. Ltd., Nanjing 210000, China. [4]Laboratory of Emerging Animal Diseases, One Health Center, College of Veterinary Medicine, Nanjing Agricultural University, Nanjing 210095, Jiangsu Province, China. [5]Tiyun Han, Guilai Liu and Chenyi Bao contributed equally to this work. ✉email: xushi@therarna.cn; maqingbo@nrp-pet.cn; yqian@njau.edu.cn

shown potential in improving immune responses against tumors[11–13]. Protein-based vaccines, such as those targeting tumor-associated antigens or immune checkpoint molecules, have been extensively studied[14]. Peptide vaccines, offering advantages in specificity and ease of manufacture, have been explored for targeting various aspects of the TME, including indoleamine 2,3-dioxygenase 1 (IDO1), programmed cell death ligand 1 (PD-L1), arginase 1 (ARG1), C-C motif chemokine ligand 22 (CCL22) and Galectin-3 and yielded encouraging results in certain cancer types[15–20]. However, while these single-target approaches have provided valuable insights and shown some efficacy, they often fall short in addressing the multifaceted nature of TME-mediated immunosuppression. The complex interplay between different immunosuppressive cell populations suggests that a more comprehensive, multi-targeted approach may be necessary to achieve robust and durable anti-tumor immune responses.

mRNA-lipid nanoparticle (LNP) technology has emerged as a promising modality, offering unparalleled flexibility in targeting multiple immunosuppressive cell populations simultaneously[21–24]. This platform allows for the simultaneous delivery of multiple mRNA sequences encoding various antigens and immunomodulatory factors, all encapsulated within a single LNP formulation. The LNP delivery system ensures efficient cellular uptake and expression of the encoded antigens and factors, enhancing the vaccine's potency. Developing a multi-targeted immunomodulatory vaccine based on the mRNA-LNP platform should offer significant advantages over single-target strategies. By eliciting an immune response against the immunosuppressive cells within tumors, the vaccine may orchestrate a comprehensive remodeling of the TME and create a more favorable environment for effective anti-tumor immune responses.

In this study, we investigate a novel mRNA-lipid nanoparticle (LNP) based immunomodulatory vaccine designed to reprogram key cellular mediators of immune suppression within the TME. The vaccine targets a comprehensive panel of immunosuppressive factors, including CCL22, transforming growth factor-β (TGF-β), cytotoxic T-lymphocyte-associated protein 4 (CTLA-4), Galectin-3, PD-L1, IDO1, and ARG1, which are pivotal in tumor immune evasion. To enhance the translational relevance of our findings, we leveraged the spontaneously occurring canine cancer model, which exhibits remarkable homology with human malignancies in terms of genetic aberrations, molecular pathways, and therapeutic responses. Preliminary results from our clinical study in canine cancer patients demonstrate that the mRNA-LNP immunomodulatory vaccine exhibited a good safety profile and significantly delayed the tumor progression in multiple cancers. This marked improvement is likely attributable to the vaccine's multifaceted approach in targeting the immunosuppressive TME. These findings not only validate the potential of mRNA-based immunotherapies in recalibrating the TME to favor anti-tumor immunity, but also demonstrate the broad application of immunomodulatory vaccines across cancer types. The therapeutic efficacy observed in this canine model would provide a strong rationale for further investigation and potential translation to human clinical trials.

Material and method

Study design and canine patient recruitment

This open-label, single-arm pilot study enrolled canine patients with histologically confirmed malignancies, adhering to stringent inclusion and exclusion criteria designed to ensure scientific rigor and patient safety. Eligible subjects met the following criteria: (i) presence of inoperable or owner-declined surgical intervention for malignancies; (ii) no prior exposure to immunosuppressive agents within one month of vaccine administration; (iii) absence of autoimmune disease history; (iv) a life expectancy > 3 month; and (v) a minimum four-week washout period from chemotherapy or immunotherapy, or six weeks from radiotherapy. Exclusion criteria encompassed: (i) unauthorized administration of immunosuppressive agents during the study period; (ii) known history of immunodeficiency virus infection; (iii) presence of active systemic infections requiring treatment; (iv) concurrent participation in other anticancer or experimental therapies; and (v) pregnancy or lactation. The study was approved by the institutional animal care and use committee (IACUC number: AB20230810) at Ai-Bi pet hospital, conducted following ARRIVEreporting guidelines[25] and informed consent was obtained from all owners.

Plasmid construction

The pUC57 vector (Genscript) for mRNA transcription in vitro was used for plasmid construction. Two novel constructs were designed: Canine-CTCG and Canine-PIA. Canine-CTCG encodes a polyantigen comprising CCL22, TGF-β, CTLA-4, and Galectin-3, while Canine-PIA encompasses PD-L1, IDO1, and ARG1. Based on the established correlation between peptide hydrophobicity and immunogenicity, we preferentially selected hydrophobic residues as the immunogenic epitopes for each antigen. These fragments were subsequently cloned into the pUC57 vector using a seamless cloning strategy. The resulting plasmids were verified by restriction analysis and Sanger sequencing to ensure the fidelity of the inserts and regulatory elements.

mRNA synthesis and purification in vitro

mRNAs were transcribed from linearized plasmids by the MEGAscript® T7 Transcription Kit through a modified protocol. Concurrently, mRNA was capped at the 5' terminus using the trinucleotide cap1 analog CleanCap (Cat# N-7413, TriLink). Following a 6-h incubation period, the transcription products were selectively precipitated using lithium chloride. The resulting mRNA pellet was dissolved in nuclease and endotoxin free water. The concentration and purity of mRNAs were detected using nanodrop and capillary electrophoresis, respectively. The final product was aliquoted and stored at − 80 °C.

mRNA-LNP production

Microfluidic technology was employed to encapsulate messenger RNA (mRNA) within lipid nanoparticles. In brief, lipids were dissolved at a molar ratio of 50:10:38.5:1.5 (SM102: DSPC: cholesterol: DMG-PEG2000) and

mRNA was prepared in 20 mM sodium acetate buffer (pH5.5) a concentration of 0.1 mg/mL. Then the lipid and mRNA solutions were mixed at an N/P ratio of 6 through the microfluidic cartridge at a total flow rate of 6 ml/min with a flow rate ratio of 3:1 (aqueous phase: organic phase). The mRNA-LNP formulation was then subjected to triplicate dialysis against 20 mM Tris–HCl buffer (pH 7.4) using a 3.5 kDa molecular weight cut-off Slide-A-Lyzer dialysis cassette. The final mRNA-LNP preparation was adjusted to a concentration of 100 μg/ml with 10% sucrose (w/v) and aliquoted for different storage conditions.

mRNA-LNP characterization

The mRNA encapsulation efficiency was determined by Quant-iTTM RiboGreen assay (Cat# R11490, Life Technologies). Encapsulation efficiency was quantified via the Quant-iT RiboGreen assay, comparing fluorescence (λex/em = 485/528 nm) in the presence and absence of Triton X-100. A standard curve was generated using known mRNA concentrations. Particle size distribution and zeta potential (ZP) was analyzed by Dynamic Lighter Scattering (DLS) instrument (DynaPro NanoStar, Wyatt Technology). Measurements were performed in PBS with or without 10% sucrose at 25 °C. Each DLS data point represents the average of four independent readings, each comprising 10 acquisitions.

Vaccine administration

The mRNA vaccine consisted of two constructs: canine-CTCG and canine-PIA. The vaccine was administered via bilateral subcutaneous injections in close proximity to the inguinal lymph nodes. Specifically, 25 μg of canine-CTCG was injected near the left inguinal lymph node, while 25 μg of canine-PIA was administered adjacent to the right inguinal lymph node, yielding a total dose of 50 μg per vaccination event. The immunization regimen includes priming doses administered on days 0, 4, 7, 14 and 28 to rapidly establish a robust immune response and booster vaccinations given at two-week intervals until disease progression or unacceptable toxicity. All vaccine administrations were performed by licensed veterinarians in strict adherence to ethical guidelines for animal research. No euthanasia was performed as this study did not involve any terminal procedures. All participating dogs remained under the care of their owners throughout and after the study period.

Clinical assessments

Patients underwent physical examinations, complete blood counts, serum biochemistry, and diagnostic imaging at baseline and at predetermined intervals post-vaccination. Adverse events were graded according to the Veterinary Cooperative Oncology Group—Common Terminology Criteria for Adverse Events (VCOG-CTCAE) v2.0.

Tumor response evaluation

Tumor responses were assessed using the Response Evaluation Criteria in Solid Tumors (cRECIST v1.0) guidelines adapted for canine patients[26]. Complete response (CR), partial response (PR), stable disease (SD), and progressive disease (PD) were defined according to these criteria.

Hematological and biochemical analyses

Complete blood counts were performed using an automated hematology analyzer (ProCyte Dx, IDEXX). Serum biochemistry panels were analyzed using a clinical chemistry analyzer (Cobas 8000, Roche Diagnostics). Reference ranges were established based on breed-specific and laboratory-specific normal values.

Diagnostic imaging

Computed tomography (CT) scans were performed using a multi-detector CT scanner (Aquilion ONE, Canon Medical Systems) with and without intravenous contrast. Ultrasound examinations were conducted using an ultrasound scanner with digital storage capacity a high-frequency linear transducer (Vivid, General Electric). Radiographs were obtained using a digital radiography system (CXDI-710C Wireless, Canon Medical Systems).

Statistical analysis

Survival analyses were performed using the Kaplan–Meier method. Progression-free survival (PFS) was defined as the time from treatment initiation to disease progression. Descriptive statistics were used for demographic data and adverse event reporting. All analyses were performed using GraphPad Prism version 9.0.

Data availability

All data generated or analyzed during this study are included in this article and its supplementary information files. No datasets were generated or analyzed during the current study. Data are available from the authors upon reasonable request.

Results

Design and characterization of a multi-targeted immunomodulatory mRNA-LNP vaccine platform

To disrupt the suppressive tumor immune environment, we developed a novel multi-targeted immunomodulatory vaccine utilizing the mRNA-LNP platform (Fig. 1A). The mRNA payload was engineered to encode a carefully curated series of immunomodulatory antigens, including CCL22, TGF-β, CTLA-4, Galectin-3, PD-L1, IDO1, and ARG1. These targets were strategically selected to address multiple immunosuppressive mechanisms within the tumor microenvironment, with a specific focus on modulating the activities of Tregs, MDSCs, and TAMs. Leveraging the established correlation between peptide hydrophobicity and immunogenicity[27], we preferentially selected hydrophobic residues as the immunogenic epitopes for each antigen. These immunogenically optimized

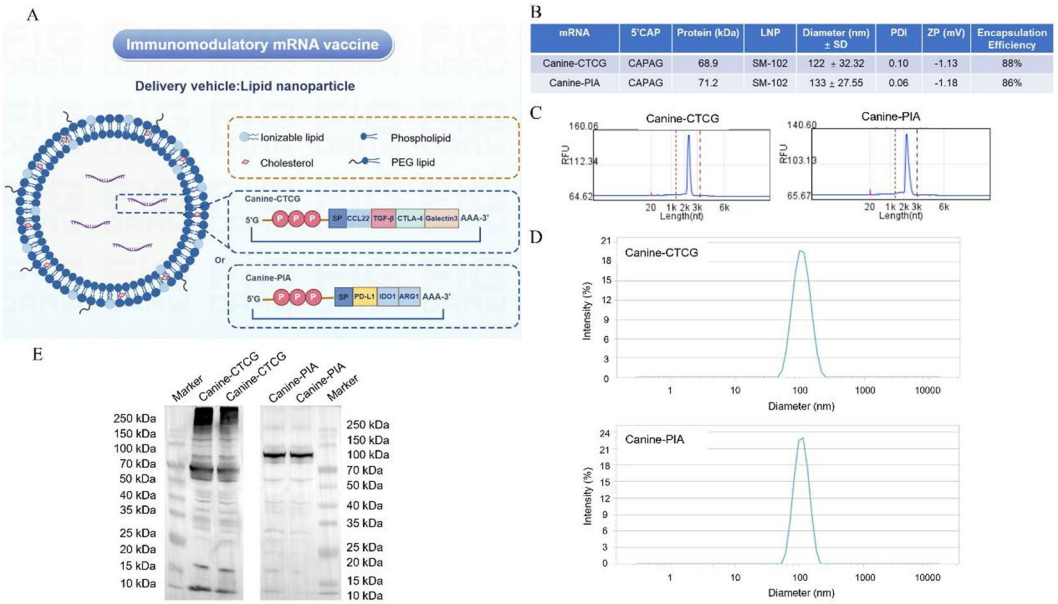

mRNA	5'CAP	Protein (kDa)	LNP	Diameter (nm) ± SD	PDI	ZP (mV)	Encapsulation Efficiency
Canine-CTCG	CAPAG	68.9	SM-102	122 ± 32.32	0.10	-1.13	88%
Canine-PIA	CAPAG	71.2	SM-102	133 ± 27.55	0.06	-1.18	86%

Fig. 1. Development and validation of a multi-targeted immunomodulatory mRNA-LNP vaccine. (**A**) Schematic representation of the mRNA-LNP vaccine design. The LNP (formulation SM-102) structure encapsulates the mRNA payload, comprising ionizable lipids, phospholipids, cholesterol, and PEG-lipids. The mRNA construct includes 5' and 3' UTRs, a signal peptide, and a series of truncated epitopes forming a minigene encoding multiple immunomodulatory antigens. Two mRNA-LNP vaccines were constructed: Canine-CTCG, encoding CCL22, TGF-β, CTLA-4, and Galectin-3; and Canine-PIA, encompassing PD-L1, IDO1, and ARG1. (**B**) Physicochemical characteristics of Canine-CTCG and Canine-PIA formulations, including mRNA content, 5'CAP, molecular weight of protein, LNP diameter, PDI, and ZP. (**C**) Capillary electrophoresis analysis for the indicated mRNA. (**D**) Particle size distribution of indicated LNP/mRNA complexes. (**E**) Western blot analysis of protein expression from Canine-CTCG and Canine-PIA constructs, with two lanes for each mRNA construct in parallel samples.

epitopes were then concatenated to construct a minigene mRNA vaccine. Due to the capacity limitations inherent to the mRNA-LNP system, we developed two distinct vaccine constructs: Canine-CTCG, encoding CCL22, TGF-β, CTLA-4, and Galectin-3; and Canine-PIA, encompassing PD-L1, IDO1, and ARG1. This allowed for comprehensive coverage of our target antigens while maintaining optimal mRNA length and stability. The vaccine formulation employed the ionizable lipid SM-102 in the LNP composition, given its established efficacy in mRNA delivery and favorable safety profile, thereby enhancing the potential for efficient antigen expression in vivo.

In vitro validation of the vaccine constructs demonstrated both favorable physicochemical properties and robust antigen expression (Fig. 1B). The results of the mRNA integrity assay showed that the purities of the Canine-CTCG and Canine-PIA mRNA constructs were 88.0% and 90.7%, respectively (Fig. 1C). The encapsulation efficiencies of the LNP for the two mRNA were 88% and 86%, respectively. DLS analysis revealed that the two formulations exhibited optimal nanoparticle characteristics, with mean diameters of 122 nm and 133 nm (Fig. 1D), respectively. Notably, both formulations displayed remarkably low polydispersity indices (PDI) of 0.10 and 0.06, indicative of highly uniform particle size distributions, which are crucial for consistent cellular uptake and antigen presentation. Western blot analysis, facilitated by the strategic incorporation of a His-tag in our constructs, provided compelling evidence of successful antigen expression (Fig. 1E and Fig. S1). The immunoblots revealed distinct bands at the expected molecular weights for both Canine-CTCG and Canine-PIA constructs, confirming the accurate translation of our engineered minigenes.

The novel immunomodulatory mRNA vaccine was well-tolerated in canine patients

To evaluate the therapeutic efficacy of our novel immunomodulatory mRNA vaccine, we initiated a pilot study to assess its safety and efficacy in canine cancer patients. The intervention consisted of subcutaneous injections of a combination of canine-CTCG and canine-PIA vaccines (25 μg each, total 50 μg) administered bilaterally in the inguinal region proximal to the lymph nodes at each immunization. As illustrated in Fig. 2A, the vaccination schedule comprised a prime phase with injections on day 0, 4, 7, 14, and 28, followed by a boost phase with injections every two weeks. This regimen was designed to induce a robust and sustained immune response against multiple tumor-associated immunosuppressive factors.

The study enrollment process is depicted in Fig. 2B. Initially, 13 canines (2 male, 11 female) were screened for eligibility. Three were excluded due to hematologic malignancy (n = 2) or chronic heart failure (n = 1). The remaining 10 dogs were enrolled and received the intervention. During the follow-up period, two discontinued the intervention for undisclosed reasons. Ultimately, 8 dogs completed the full treatment course and were

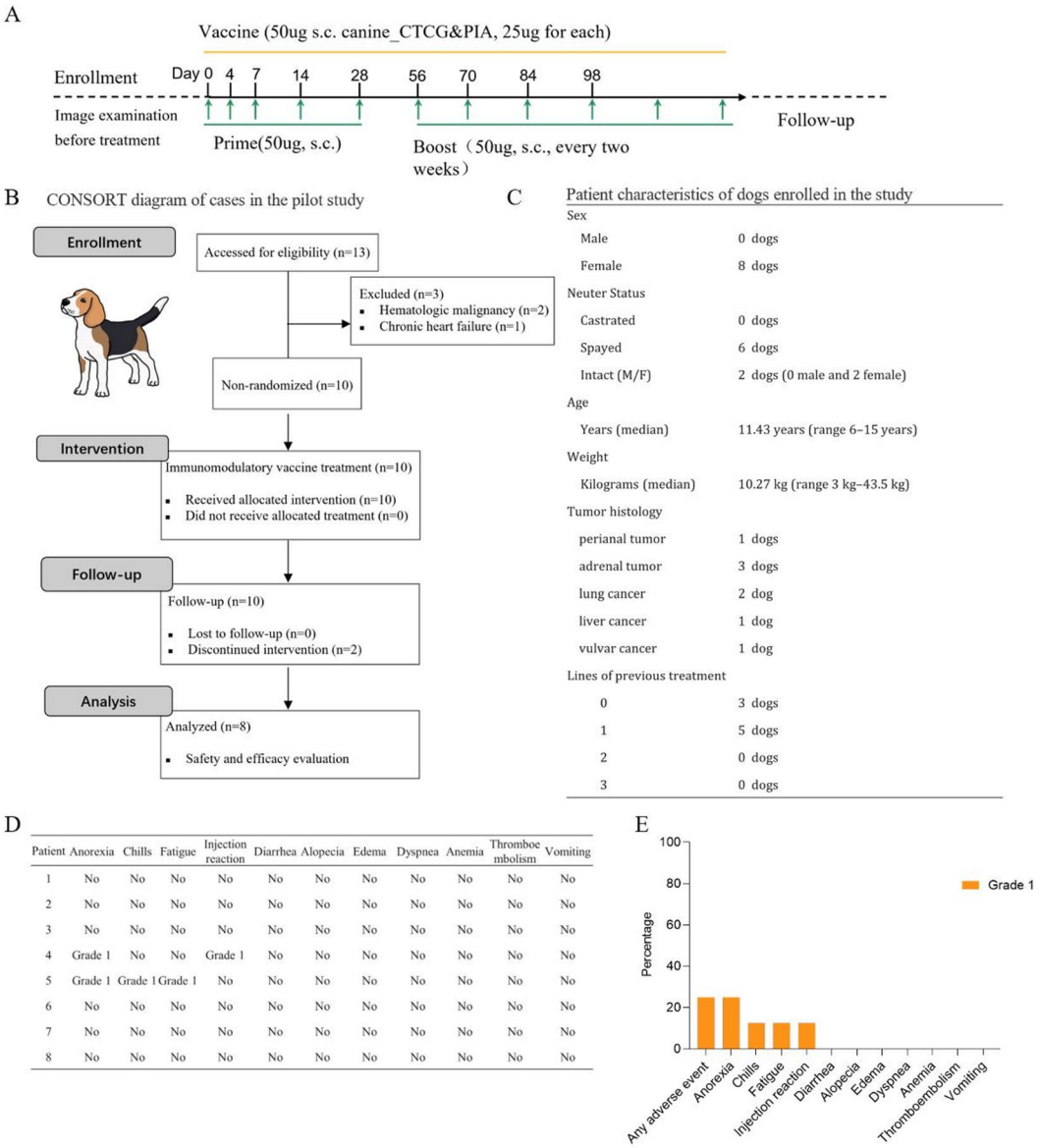

Patient	Anorexia	Chills	Fatigue	Injection reaction	Diarrhea	Alopecia	Edema	Dyspnea	Anemia	Thromboembolism	Vomiting
1	No	No	No	No	No	No	No	No	No	No	No
2	No	No	No	No	No	No	No	No	No	No	No
3	No	No	No	No	No	No	No	No	No	No	No
4	Grade 1	No	No	Grade 1	No	No	No	No	No	No	No
5	Grade 1	Grade 1	Grade 1	No	No	No	No	No	No	No	No
6	No	No	No	No	No	No	No	No	No	No	No
7	No	No	No	No	No	No	No	No	No	No	No
8	No	No	No	No	No	No	No	No	No	No	No

Fig. 2. Study design, canine patient characteristics, and safety profile of the novel immunomodulatory mRNA vaccine. (**A**) Schematic representation of the intervention regimen. The mRNA vaccine, comprising canine_ CTCG and PIA (25 μg each), was administered subcutaneously. The regimen included a prime dose (50 μg) at day 0, 4, 7, 14, and 28, followed by boost doses (50 μg) every two weeks. (**B**) A diagram illustrating patient flow through the pilot study. Of 13 dogs initially assessed, 10 were enrolled, with 8 completing the full course of treatment and included in the final analysis. (**C**) Demographic and clinical characteristics of the study cohort (n = 8). The table summarizes sex distribution, neuter status, age, weight, tumor histology, and prior treatment history. (**D**) Comprehensive adverse event profile for each patient (n = 8). Events were graded according to standard toxicity criteria VCOG-CTCAE v2. The majority of patients experienced no adverse events, with only mild (Grade 1) events observed in two patients. (**E**) Bar graph depicting the frequency of adverse events across the study population. The y-axis represents the percentage of dogs experiencing each event type, stratified by severity grade.

included in the final safety and efficacy analysis. The final cohort comprised a diverse array of breeds: three Toy Poodles (Canis lupus familiaris f. canis), two Chinese Rural Dogs (Canis lupus familiaris), one Pomeranian (Canis lupus familiaris f. pomeranus), one Chihuahua (Canis lupus familiaris f. chihuahua), and one Golden Retriever (Canis lupus familiaris f. retriever). The individual canine patient demographics and a comprehensive overview of the patient characteristics are shown in Table 1 and Fig. 2C. The study cohort predominantly consisted of female dogs (n = 8), with a median age of 11.43 years (range 6–15 years) and a median weight of 10.27 kg (range 3–43.5 kg). Tumor histology was diverse, encompassing perianal tumor (n = 1), adrenal tumor (n = 3), lung cancer (n = 2), liver cancer (n = 1), and vulvar cancer (n = 1), demonstrating the potential broad

No	Age(years)	Sex	Weight (kg)	Neuter Status	Diagnosis	Anatomical tumor location	Benign/Malignant	Previous treatment	Disease progression before vaccination
1	9.5	Female	4.5	Sprayed	Perianal tumor	Perianal	Malignant	No	Perianal mass, hind limb pain, gait unsteadiness
2	12	Female	8	Sprayed	Adrenal tumor	Bilateral adrenal glands	Malignant	Trilostane	Bilateral adrenal enlargement, polydipsia, polyuria, erythrocytosis
3	14	Female	11	Sprayed	Liver cancer	Liver	Malignant	Surgery	Recurrence post suregery
4	13	Female	3	No	Adrenal tumor	Right adrenal gland	Malignant	Trilostane	Right adrenal enlargement, polydipsia, polyuria, erythrocytosis
5	11	Female	3	Sprayed	Vulvar cancer	Vulvar	Malignant	Surgery	Recurrence post surgery
6	11	Female	5.5	Sprayed	Lung cancer	Lung	Malignant	Surgery	Recurrence post surgery
7	12	Female	3.4	Sprayed	Adrenal tumor	Left adrenal gland	Malignant	No	Left adrenal enlargement, polydipsia, polyuria
8	6	Female	43.5	No	Lung cancer	Lung	Malignant	No	Primary lung cancer

Table 1. Individual canine patient demognpbia.

applicability of the vaccine across various neoplastic conditions. The majority of dogs (n = 5) had received one line of previous treatment, while three dogs were treatment-naïve.

Safety evaluation was a primary focus of this study. The adverse event profile was remarkably favorable, with the majority of dogs experiencing no treatment-related side effects (Fig. 2D and E). Of the 8 dogs analyzed, only two (Patient 4 and 5) exhibited some adverse events, which were limited to Grade 1 anorexia, chills, and fatigue. Importantly, no severe adverse events (Grade 2 or higher) were observed throughout the study period, highlighting the overall safety of the vaccine regimen. The low incidence and mild nature of the observed side effects are particularly encouraging, considering the novel nature of the mRNA vaccine and the fragile health status often associated with cancer-bearing dogs. This safety profile suggests that the combination of canine-CTCG and canine-PIA vaccines, delivered via the described administration protocol, is well-tolerated and could potentially be suitable for broader clinical application in canine oncology.

The immunomodulatory mRNA vaccine demonstrated durable therapeutic efficacy across multiple cancers

The efficacy of the novel canine cancer immunotherapy vaccine was evaluated in eight dogs with various tumor types, as illustrated in Fig. 3. Notably, five out of eight dogs (62.5%) exhibited stable disease for extended periods, ranging from approximately 120–250 days (Fig. 3A). Three dogs (37.5%) with perianal tumor or lung cancer experienced disease progression. Importantly, no treatment-related deaths were observed during the study period. The diversity of tumor types responding to the vaccine, including adrenal, liver, and vulvar cancers, suggests a potentially broad applicability of this immunotherapeutic approach across different canine malignancies.

While no complete responses (CR) or partial responses (PR) were observed, a remarkable 75% (6/8) of the dogs achieved stable disease (SD), indicating a notable disease control rate (Fig. 3B). The remaining 25% (2/8) experienced progressive disease (PD). The disease control rate (DCR), encompassing SD, PR, and CR, was 75%, highlighting the vaccine's potential to stabilize diverse cancer types in canines. Importantly, the median progression-free survival (PFS) has not been reached during the study period, suggesting durable responses in a significant proportion of treated animals. The Kaplan–Meier curves for progression-free survival demonstrates that over 60% of dogs remained progression-free, ranging from 126 to 252 days (Fig. 3C), corroborating the extended stable disease observed in Fig. 3A. The overall survival curve indicates a clear separation between those with stable disease and those experiencing progression (Fig. 3D). These survival data, albeit from a small cohort, suggest promising durability of the vaccine's effect and potential long-term benefit in canine cancer patients.

Vaccine administration reverses hematological and biochemical abnormalities in canine patients

To assess the physiological changes in dogs' post-vaccine administration, we collected blood samples and performed comprehensive hematological and biochemical analyses. The hematological profiles of canine patients treated with the novel cancer immunotherapy vaccine demonstrate significant improvements across various parameters, as illustrated in Fig. 4. Patient 1, diagnosed with a perianal tumor, exhibited notable changes post-treatment. The lymphocyte (LYM) and monocyte (MONO) counts increased, suggesting enhanced immune system activation (Fig. 4A). Concurrently, a decrease in neutrophil count was observed, potentially reflecting a shift from acute inflammation to a more regulated immune response. Patient 2, presenting with an adrenal tumor, showed amelioration of erythrocytosis, a common paraneoplastic syndrome associated with adrenal tumors (Fig. 4B). The hemoglobin (HGB) levels decreased towards normal range, while REITIC increased, indicating a more balanced erythropoiesis. The normalization of elevated platelet counts suggests a reduction in tumor-associated thrombocytosis. Patient 4, also with an adrenal tumor, demonstrated similar improvements in erythrocytosis and thrombocytosis (Fig. 4C). However, this patient exhibited a decrease in lymphocytes with increases in monocytes and eosinophils, potentially reflecting a distinct immune response pattern. Patient 7, another adrenal tumor case, showed resolution of leukocytosis and thrombocytosis, with increases in lymphocytes and eosinophils, and a decrease in monocytes (Fig. 4D). These hematological shifts across different tumor types suggest that the vaccine therapy may be modulating the immune system and addressing paraneoplastic syndromes, regardless of the primary tumor site.

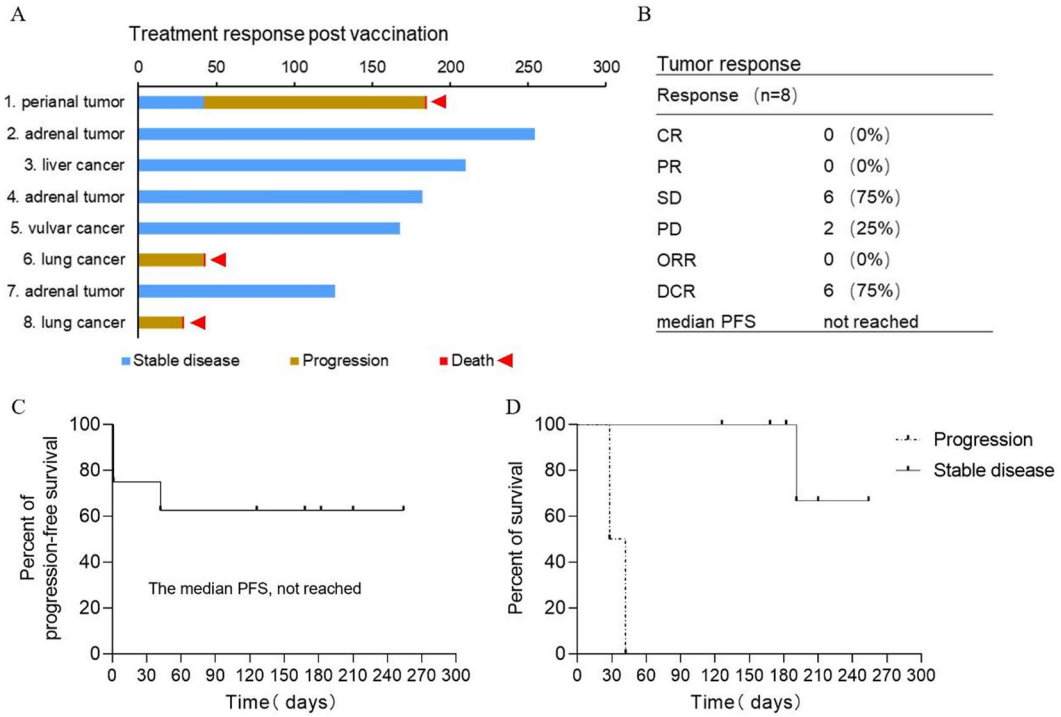

Fig. 3. Treatment response and survival analysis of canine cancer patients treated with the novel immunotherapy vaccine. (**A**) Swimmer plot depicting individual treatment responses post-vaccination. Each bar represents a single patient, with colors indicating disease status: blue for stable disease, yellow for progression, and red for death marked with red arrow. The x-axis shows days post-treatment initiation. Diverse tumor types, including perianal, adrenal, liver, vulvar, and lung cancers, demonstrate varied response durations. (**B**) Summary of tumor responses (n = 8). CR: complete response; PR: partial response; SD: stable disease; PD: progressive disease; ORR: objective response rate; DCR: disease control rate; PFS: progression-free survival. (**C**) Kaplan–Meier curve for progression-free survival (PFS). (**D**) Kaplan–Meier curve for overall survival, stratified by disease status (progression vs. stable disease).

The biochemical profiles of the treated canine patients reveal significant alterations in various metabolic and organ function parameters, providing insights into the systemic effects of both the tumors and the immunotherapy (Fig. 5). Patient 1, with a perianal tumor, exhibited a decrease in alanine aminotransferase (ALT), which may indicate a shift in liver enzyme activity, possibly related to treatment response (Fig. 5A). Notably, the initially elevated C-reactive protein (CRP) levels improved, suggesting a reduction in systemic inflammation post vaccination. Patient 2, diagnosed with an adrenal tumor, showed marked improvements in several parameters (Fig. 5B). The initially elevated creatinine and urea nitrogen levels normalized, indicating enhanced renal function. A complete resolution of elevated alkaline phosphatase (ALKP) was observed, which is particularly significant given the frequent elevation of this enzyme in adrenal tumors. The decrease in total CO_2 (TCO2) suggests improved acid–base balance, while the normalization of CREA levels further supports a reduction in systemic inflammation. Patient 4, also with an adrenal tumor, demonstrated improvement in aspartate aminotransferase (AST) levels, suggesting partial resolution of hepatocellular injury (Fig. 5C). The ALKP levels also showed improvement, consistent with the response seen in patient 2. Patient 7, the third adrenal tumor case, exhibited improved globulin levels (Fig. 5D). The marked improvements in ALKP and TCO2 levels were observed, aligning with the responses seen in other adrenal tumor patients. These biochemical changes, when considered in the context of each tumor type, suggest that the vaccine therapy may be not only exerting anti-tumor effects by modulating the immune response but also alleviating paraneoplastic syndromes associated with these malignancies.

Ultrasound evidence of tumor response to vaccination therapy in hepatic and adrenal neoplasms

Ultrasound imaging plays a crucial role in evaluating treatment responses in oncology, offering real-time, non-invasive visualization of tumor morphology and dimensions. In this study, we present comparative ultrasound findings from patients with liver cancer, adrenal and perianal tumors to elucidate the differential responses to our novel vaccination therapy. These cases were selected to demonstrate the spectrum of treatment outcomes, including significant stable disease and progression, and to provide insight into the varied efficacy of immunotherapeutic approaches across different tumor types.

For liver cancer (Patient 3), ultrasound images reveal a remarkable reduction in liver tumor dimensions following vaccination therapy (Fig. 6A and B). Pre-treatment imaging shows a well-defined hypoechoic mass

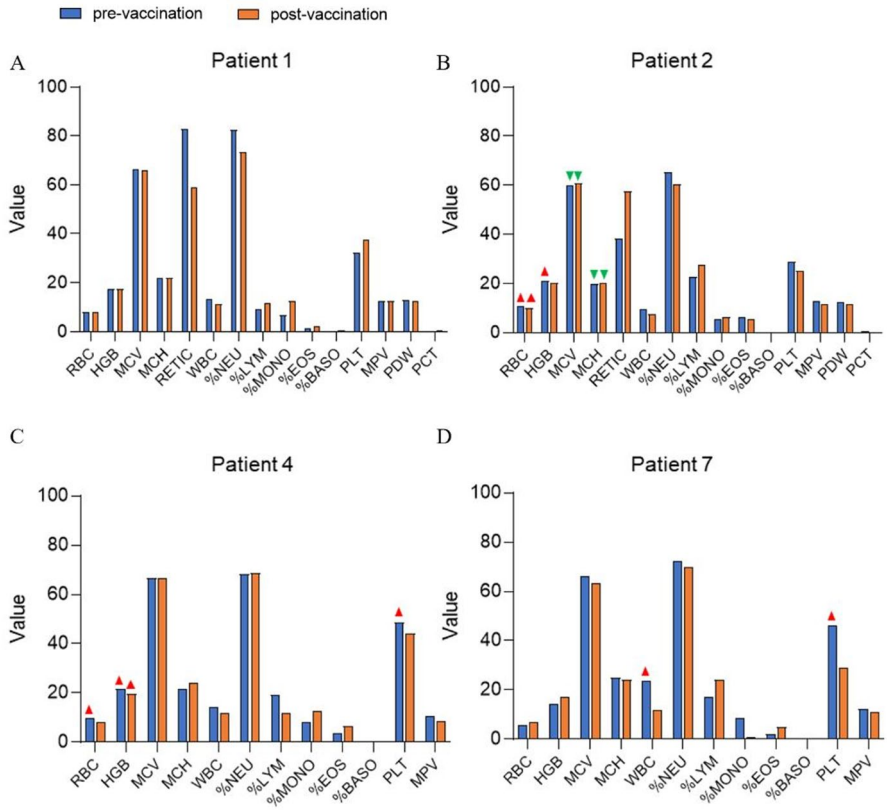

Fig. 4. Hematological profiles of canine cancer patients pre- and post- immunotherapy vaccination. (**A**–**D**) Hematological parameters for patient 1, 2, 4, and 7. Blue bars represent pre-treatment values, and orange bars represent post-treatment values. Red triangles indicate values above the normal range, while green triangles indicate values below the normal range. Key parameters include red blood cell (RBC, unit: 10^{12}/L) count, hemoglobin (HGB, unit: g/dL), mean corpuscular volume (MCV, unit: fL), mean corpuscular hemoglobin (MCH, unit: pg), reticulocyte index (REITIC, unit: K/μL), white blood cell (WBC, unit: 10^9/L) count, neutrophils (NEU, unit: %), lymphocytes (LYM, unit: 10^9/L) count, monocytes (MONO, unit: 10^9/L), eosinophils (EOS, unit: 10^9/L) count, basophils (BASO, unit: 10^9/L) count, platelets (PLT, unit: K/μL), mean platelet volume (MPV, unit: fL), platelet distribution width (PDW, unit: fL), plateletcrit (PCT, unit: %).

measuring 1.8 cm × 2.4 cm within the hepatic parenchyma. The lesion appears heterogeneous with irregular margins, characteristics typical of malignant hepatic neoplasms. Histopathological examination reveals a densely cellular neoplasm that has completely effaced the normal hepatic architecture (Fig. S2). Notably absent are the quintessential features of normal liver tissue, including portal triads, central veins, and the typical radiating pattern of hepatic cords. This architectural disruption is a hallmark of malignant transformation in liver tissue. The neoplastic hepatocytes display striking cytological atypia. These cells are predominantly large and polygonal, with abundant cytoplasm exhibiting a distinctive vacuolar appearance. They contain variably sized, round to oval vesicular nuclei with prominent nucleoli. Mitotic figures are frequently observed, averaging 0–2 per high-power field. The hepatocytes show moderate anisokaryosis and anisocytosis, with bi- to tri-nucleation observed. Multifocally, the sinusoids are variably dilated and filled with erythrocytes, indicative of peliotic change. Post-vaccination imaging of the same region demonstrates a significant decrease in tumor size, with new dimensions of 1.72 cm × 2.11 cm. This represents a volume reduction of approximately 26%, suggesting a positive response to the vaccine-based intervention. The post-treatment image also shows subtle changes in the lesion's echotexture, possibly indicating areas of tumor necrosis or fibrotic transformation.

Contrastingly, the adrenal tumor (Patient 2) exemplifies a case of stable disease (Fig. 6C and D). The pre-vaccination image shows a well-circumscribed, hypoechoic mass within the adrenal gland, measuring 1.04 cm × 1.08 cm. The lesion's homogeneous appearance and clear delineation from surrounding tissues are consistent with an adrenal adenoma or early-stage carcinoma. Post-vaccination, a modest reduction in tumor size is observed, with new dimensions of 0.8 cm × 1.2 cm. While the change in tumor volume is less pronounced than in Patient 3, there is a noticeable alteration in the lesion's internal architecture, with areas of increased echogenicity potentially signifying treatment-induced changes in tumor composition.

In contrast to the above cases, Patient 1, diagnosed with a perianal tumor, exhibited disease progression despite initial clinical improvement (Fig. S3). CT imaging revealed an irregular, infiltrative mass in the left perianal region, with poorly defined borders interfacing with the rectum and surrounding soft tissues (Fig. S3A). This invasive growth pattern, characteristic of aggressive perianal tumors, poses significant challenges for local

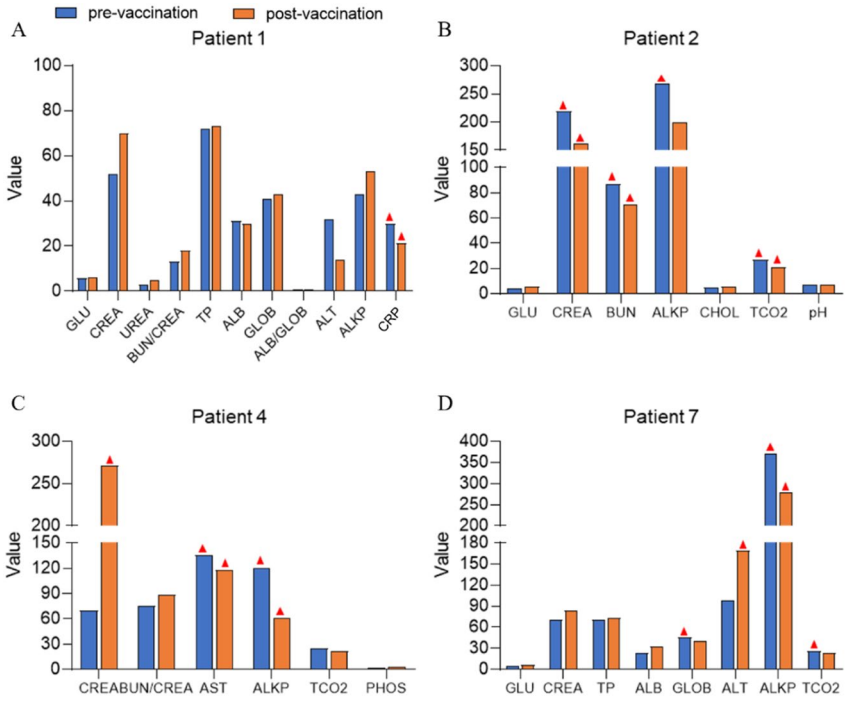

Fig. 5. Biochemical profiles of canine cancer patients before and after immunotherapy vaccination. (A-D) Biochemical parameters for patient 1, 2, 4, and 7. Red triangles indicate values above the normal range. Abbreviations: GLU (glucose, unit: mmol/L), CREA (creatinine, unit: μmol/L), BUN (blood urea nitrogen), ALKP (alkaline phosphatase, unit: U/L), CHOL (cholesterol, unit: mmol/L), TCO2 (total CO_2, unit: mmol/L), AST (aspartate aminotransferase, unit: U/L), ALT (alanine aminotransferase, unit: U/L), TP (total protein, unit: g/L), ALB (albumin), GLOB (globulin, g/L), CRP (C-reactive protein, unit: mg/L), PHOS (Phosphate, unit: mmol/L).

control. Enlarged internal and external iliac lymph nodes suggest lymphatic metastasis, while apparent invasion of caudal vertebral tissues indicates advanced local progression. Ultrasound imaging of the perianal tumor mass showed an increase from 5.41 cm to 6.67 cm in diameter post-treatment (Fig. S3B and C). Despite an initial period of clinical improvement during the first month of treatment, characterized by enhanced mobility and overall demeanor, the patient subsequently experienced disease progression manifesting as left hind limb edema and fracture, likely due to tumor invasion of the skeletal structure.

These ultrasound findings provide valuable insights into the differential responses of hepatic, adrenal, and perianal tumors to vaccination therapy. The more substantial reduction in the hepatic tumor size suggests a potentially higher susceptibility of liver neoplasms to this innovative treatment approach. Conversely, the adrenal tumor's more modest response and the progression of the perianal tumor highlight the variability in treatment efficacy across different tumor types and anatomical locations. These observations underscore the importance of personalized medicine approaches in cancer immunotherapy and the need for further investigation into the mechanisms underlying differential tumor responses to vaccination strategies.

Discussion

This study presents compelling evidence for the safety and potential efficacy of a novel immunomodulatory mRNA vaccine in the treatment of diverse canine cancers. The comprehensive analysis of hematological, biochemical, and clinical responses, coupled with survival outcomes, provides a multifaceted view of the vaccine's impact on canine cancer patients. The observed safety profile, characterized by a low incidence of mild adverse events and absence of severe toxicities, is particularly encouraging and aligns with findings from human trials of similar immunomodulatory approaches[15,20]. The ability to induce stable disease in 62.5% of treated dogs across various tumor types, including adrenal, liver, vulvar, and lung cancers, indicates a potentially broad applicability of this immunotherapeutic approach. This non-specific anti-tumor activity is a hallmark of successful immunotherapy and suggests that the vaccine may be exerting effects by activating and modulating the immune system, similar to observations in studies targeting IDO1, PD-L1, and other immune checkpoints[17–19].

The hematological and biochemical changes observed post-treatment provide intriguing insights into the vaccine's mechanism of action and its systemic effects. The normalization of several parameters, such as the resolution of erythrocytosis and thrombocytosis in adrenal tumor cases, and the modulation of lymphocyte, monocyte, and eosinophil counts across different tumor types, suggests that the vaccine may be addressing both the primary tumors and their associated paraneoplastic syndromes. These changes not only contribute to the overall well-being of the patients but may also create a more favorable immune environment for anti-tumor

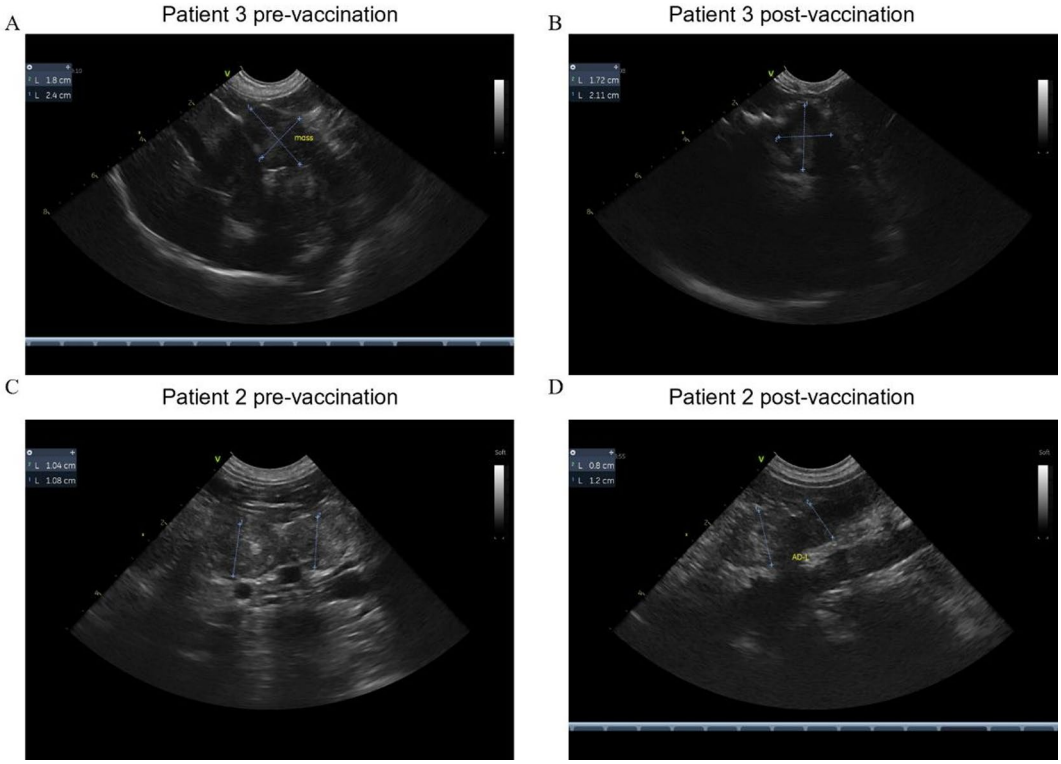

Fig. 6. Ultrasound imaging reveals differential tumor responses to vaccination therapy in hepatic and adrenal neoplasms. (**A**, **B**) Patient 3: Pre-vaccination (day 0) and post-vaccination (28 days after 5 doses) ultrasound of liver tumor. (**A**) Pre-vaccination image shows a hypoechoic mass measuring 1.8 × 2.4 cm. (**B**) Post-vaccination image demonstrates significant tumor shrinkage to 1.72 × 2.11 cm, representing a 26% volume reduction. (**C**, **D**) Patient 2: Pre-vaccination (day 0) and post-vaccination (3 days after 6 doses) ultrasound of adrenal tumor. (**C**) Pre-vaccination image reveals a well-defined hypoechoic mass measuring 1.04 × 1.08 cm. (**D**) Post-vaccination image shows modest size reduction to 0.8 × 1.2 cm with altered internal architecture. Scale bars represent 1 cm.

responses, reminiscent of the immune modulation observed in studies targeting regulatory T cells and myeloid-derived suppressor cells[9,10,28].

The survival analysis presents perhaps the most compelling evidence for the vaccine's potential efficacy. The median progression-free survival was not reached during the study period, with a remarkable 62.5% (5/8) of canine subjects maintaining progression-free status at the time of analysis. This sustained response, with a maximum observed PFS of 252 days, represents a significant advancement in the management of refractory canine neoplasms and warrants further investigation into the long-term efficacy of this therapeutic approach. In addition, the diversity of tumor types responding to the vaccine is particularly noteworthy, as it suggests the potential broad applicability of the vaccine across multiple cancers, mirroring the promise shown by multi-targeted approaches in human clinical trials[15,20]. Long-term follow-up is also important in demonstrating the feasibility and translational relevance of this technology platform. Specifically, we are monitoring all survival patients at regular intervals for up to 12 months. This includes: (1) Assessments for disease progression or recurrence; (2) Hematologic and biochemical evaluations to detect delayed toxicities; (3) Imaging studies where applicable; (4) Documentation of any late-onset adverse events. These efforts will enable us to evaluate the durability of disease control and the long-term safety profile of the vaccine platform.

However, it is crucial to interpret these results in the context of the study's limitations. The small sample size and the non-randomized nature of the trial necessitate caution in generalizing these findings. The heterogeneity of tumor types, while demonstrating broad applicability, also complicates the interpretation of tumor-specific responses. Although limited by the sample size, the PFS results provide a preliminary indication that only two lung cancer patients (post-surgical recurrence and primary stage) continued to have disease progression after vaccination compared to other tumor types, which may be related to the higher metastatic rate of lung cancer. The case of patient 1, who showed initial clinical improvement followed by disease progression, highlights the complex and sometimes unpredictable nature of immune-mediated anti-tumor responses. The imaging results, particularly the progression of skeletal involvement, suggest that while the vaccine may induce systemic immune responses, it may have limitations in controlling locally aggressive or metastatic disease in some cases. As expected, vaccine response results were also related to the type of tumor, progression stage and expression of target antigens. These case underscores the need for combination strategies that can address both the primary tumor and potential metastatic sites. These observations also highlight the need for further studies to identify predictive

biomarkers of response and stratify outcomes by tumor histology or site. Patient stratification in future trials will be guided by the following: (1) Tumor antigen expression profiles, including levels of key immunosuppressive mediators targeted by the vaccine, such as PD-L1, IDO1, TGF-β, CTLA-4, ARG1, CCL22, galectin-3, etc.; (2) Baseline immune status, including T cell infiltration patterns and systemic cytokine signatures; (3) HLA typing, to assess the potential for improved antigen presentation and vaccine responsiveness.

Another limitation of this study is the lack of a placebo or untreated control group, which raises the possibility that the observed clinical benefit may, in part, reflect natural disease fluctuations or placebo effects. Although spontaneous tumor stabilization is uncommon in advanced-stage canine malignancies, it cannot be completely ruled out. Also, the comparisons with historical controls from other institutions are inherently limited. Future studies will incorporate randomized, placebo-controlled designs to better isolate true therapeutic effects and strengthen the causal interpretation of the clinical and immunological results observed here.

Looking forward, this study opens several avenues for future research and clinical development. The promising safety profile and signs of efficacy warrant larger, randomized controlled trials to more definitively establish the vaccine's efficacy across different canine cancer types. Investigation into the specific immune mechanisms activated by the vaccine, including analysis of cytokines, tumor-infiltrating lymphocytes and circulating immune cell phenotypes, could provide valuable insights into its mode of action and guide strategies for enhancing its efficacy. An in-depth study of the vaccine-activated antitumor immune response mechanism will be needed after a more comprehensive clinical trial was designed and a sufficient number of eligible participants were enrolled. Exploration of combination therapies, such as pairing the vaccine with checkpoint inhibitors or conventional treatments like radiation therapy, could potentially address the limitations observed in some non-responders or in cases of locally aggressive disease. Additionally, the translation of this approach to human oncology presents an exciting possibility, given the often-conserved nature of tumor antigens between canines and humans. The relatively rapid progression of canine cancers also makes them excellent models for evaluating immunotherapy approaches, potentially accelerating the development of similar treatments for human patients.

The favorable results in canine cancer models support the potential of our mRNA-LNP vaccine for human application, but clinical translation will require specific adjustments. Dosing must be carefully recalibrated through allometric scaling and preclinical toxicology, followed by adaptive dose-escalation in early-phase human trials to ensure safety and tolerability. Initial dosing will be conservative, with close immune monitoring. Target selection in humans will be guided by profiling the tumor microenvironment to identify the most relevant immunosuppressive pathways. While our current vaccine targets seven molecules, human trials may prioritize multiple targets—based on their relevance and expression across tumor types. The modular design of the vaccine allows for flexible tailoring to patient-specific tumor profiles. From a regulatory perspective, the Good Manufacturing Practice (GMP) compliant manufacturing process and the conduct of Good Laboratory Practice (GLP) toxicology studies can support an Investigational New Drug (IND) application. The human trial should include rigorous safety monitoring, blinded imaging, and immune profiling. Long-term considerations such as manufacturing scalability, cost, and patient access will also guide future clinical development.

Conclusion

In conclusion, this novel mRNA-based cancer vaccine demonstrates significant promise in the field of veterinary oncology, potentially offering a new, well-tolerated, and broadly applicable treatment option for canine cancer patients, while also providing valuable insights that may inform human cancer immunotherapy research.

Data availability

The datasets used and analyzed during the current study are available from the corresponding author or Jing Li (li.jing@therarna.cn) on reasonable request.

Received: 24 February 2025; Accepted: 24 September 2025
Published online: 31 October 2025

References

1. Cercek, A. et al. PD-1 blockade in mismatch repair-deficient, locally advanced rectal cancer. *N. Engl. J. Med.* **386**, 2363–2376. https://doi.org/10.1056/NEJMoa2201445 (2022).
2. Forde, P. M. et al. Neoadjuvant PD-1 blockade in resectable lung cancer. *N. Engl. J. Med.* **378**, 1976–1986. https://doi.org/10.1056/NEJMoa1716078 (2018).
3. Topalian, S. L. et al. Safety, activity, and immune correlates of anti-PD-1 antibody in cancer. *N. Engl. J. Med.* **366**, 2443–2454. https://doi.org/10.1056/NEJMoa1200690 (2012).
4. VanderWalde, A. et al. Ipilimumab with or without nivolumab in PD-1 or PD-L1 blockade refractory metastatic melanoma: A randomized phase 2 trial. *Nat. Med.* **29**, 2278–2285. https://doi.org/10.1038/s41591-023-02498-y (2023).
5. van Weverwijk, A. & de Visser, K. E. Mechanisms driving the immunoregulatory function of cancer cells. *Nat. Rev. Cancer* **23**, 193–215. https://doi.org/10.1038/s41568-022-00544-4 (2023).
6. Ruffin, A. T. et al. Improving head and neck cancer therapies by immunomodulation of the tumour microenvironment. *Nat. Rev. Cancer* **23**, 173–188. https://doi.org/10.1038/s41568-022-00531-9 (2023).
7. DePeaux, K. & Delgoffe, G. M. Metabolic barriers to cancer immunotherapy. *Nat. Rev. Immunol.* **21**, 785–797. https://doi.org/10.1038/s41577-021-00541-y (2021).
8. Huang, Y. et al. Improving immune-vascular crosstalk for cancer immunotherapy. *Nat. Rev. Immunol.* **18**, 195–203. https://doi.org/10.1038/nri.2017.145 (2018).
9. Mousavi Niri, N. et al. Improved anti-treg vaccination targeting foxp3 efficiently decreases regulatory T cells in mice. *J. Immunother.* **39**, 269–275. https://doi.org/10.1097/CJI.0000000000000133 (2016).
10. Nair, S., Boczkowski, D., Fassnacht, M., Pisetsky, D. & Gilboa, E. Vaccination against the forkhead family transcription factor Foxp3 enhances tumor immunity. *Can. Res.* **67**, 371–380. https://doi.org/10.1158/0008-5472.CAN-06-2903 (2007).

11. Hassan, R. et al. Clinical response of live-attenuated, listeria monocytogenes expressing mesothelin (CRS-207) with chemotherapy in patients with malignant pleural mesothelioma. *Clin. Cancer Res. Off. J. Am. Assoc. Cancer Res.* **25**, 5787–5798. https://doi.org/10.1158/1078-0432.CCR-19-0070 (2019).
12. Chen, Y. et al. Development of a Listeria monocytogenes-based vaccine against hepatocellular carcinoma. *Oncogene* **31**, 2140–2152. https://doi.org/10.1038/onc.2011.395 (2012).
13. Andersen, M. H. The targeting of tumor-associated macrophages by vaccination. *Cell Stress* **3**, 139–140. https://doi.org/10.15698/cst2019.05.185 (2019).
14. Lin, Z. et al. A PD-L1-based cancer vaccine elicits antitumor immunity in a mouse melanoma model. *Mol. Ther. Oncol.* **14**, 222–232. https://doi.org/10.1016/j.omto.2019.06.002 (2019).
15. Lorentzen, C. L., Kjeldsen, J. W., Ehrnrooth, E., Andersen, M. H. & Marie Svane, I. Long-term follow-up of anti-PD-1 naive patients with metastatic melanoma treated with IDO/PD-L1 targeting peptide vaccine and nivolumab. *J. Immunother. Cancer* https://doi.org/10.1136/jitc-2023-006755 (2023).
16. Dey, S. et al. Peptide vaccination directed against IDO1-expressing immune cells elicits CD8(+) and CD4(+) T-cell-mediated antitumor immunity and enhanced anti-PD1 responses. *J. Immunother. Cancer* https://doi.org/10.1136/jitc-2020-000605 (2020).
17. Nandre, R. et al. IDO vaccine ablates immune-suppressive myeloid populations and enhances antitumor effects independent of tumor cell IDO status. *Cancer Immunol. Res.* **10**, 571–580. https://doi.org/10.1158/2326-6066.CIR-21-0457 (2022).
18. Bendtsen, S. K. et al. Peptide vaccination activating Galectin-3-specific T cells offers a novel means to target Galectin-3-expressing cells in the tumor microenvironment. *Oncoimmunology* **11**, 2026020. https://doi.org/10.1080/2162402X.2022.2026020 (2022).
19. Aaboe Jorgensen, M. et al. Arginase 1-based immune modulatory vaccines induce anticancer immunity and synergize with anti-PD-1 checkpoint blockade. *Cancer Immunol. Res.* **9**, 1316–1326. https://doi.org/10.1158/2326-6066.CIR-21-0280 (2021).
20. Kjeldsen, J. W. et al. A phase 1/2 trial of an immune-modulatory vaccine against IDO/PD-L1 in combination with nivolumab in metastatic melanoma. *Nat. Med.* **27**, 2212–2223. https://doi.org/10.1038/s41591-021-01544-x (2021).
21. Zong, Y., Lin, Y., Wei, T. & Cheng, Q. Lipid nanoparticle (LNP) enables mRNA delivery for cancer therapy. *Adv. Mater.* **35**, e2303261. https://doi.org/10.1002/adma.202303261 (2023).
22. Rojas, L. A. et al. Personalized RNA neoantigen vaccines stimulate T cells in pancreatic cancer. *Nature* **618**, 144–150. https://doi.org/10.1038/s41586-023-06063-y (2023).
23. Sahin, U. et al. An RNA vaccine drives immunity in checkpoint-inhibitor-treated melanoma. *Nature* **585**, 107–112. https://doi.org/10.1038/s41586-020-2537-9 (2020).
24. Kranz, L. M. et al. Systemic RNA delivery to dendritic cells exploits antiviral defence for cancer immunotherapy. *Nature* **534**, 396–401. https://doi.org/10.1038/nature18300 (2016).
25. Percie du Sert, N. H. V., Ahluwalia, A., Alam, S., Avey, M. T., Baker, M., Browne, W. J., Clark, A., Cuthill, I. C., Dirnagl, U., Emerson, M., Garner, P., Holgate, S. T., Howells, D. W., Karp, N. A., Lazic, S. E., Lidster, K., MacCallum, C. J., Macleod, M., Pearl, E. J., Petersen, O., Rawle, F., Peynolds, P., Rooney, K., Sena, E. S., Silberberg, S. D., Steckler, T. & Wurbel, H. The ARRIVE Guidelines 2.0: updated guidelines for reporting animal research.
26. Nguyen, S. M., Thamm, D. H., Vail, D. M. & London, C. A. Response evaluation criteria for solid tumours in dogs (v1.0): A veterinary cooperative oncology group (VCOG) consensus document. *Vet. Comp. Oncol.* **13**, 176–183. https://doi.org/10.1111/vco.12032 (2015).
27. Wells, D. K. et al. Key parameters of tumor epitope immunogenicity revealed through a consortium approach improve neoantigen prediction. *Cell* **183**, 818–834813. https://doi.org/10.1016/j.cell.2020.09.015 (2020).
28. Lecoq, I. et al. CCL22-based peptide vaccines induce anti-cancer immunity by modulating tumor microenvironment. *Oncoimmunology* **11**, 2115655. https://doi.org/10.1080/2162402X.2022.2115655 (2022).

Acknowledgements

This work was supported by Nanjing Agricultural University (NAU)-TheraRNA Animal mRNA Engineering Technology Center.

Author contributions

GL and TH conceptualized the study, devised the experimental approach, and wrote the original draft of the manuscript. TH designed the mRNA constructs and prepared the mRNA-LNP formulations. CB and JZ conducted vaccine administration procedures, performed hematological and biochemical analyses, and carried out diagnostic imaging. CF and JL analyzed and interpreted the data. SX, QM, and YQ supervised the project, contributed to the experimental design, and critically revised the manuscript. All authors reviewed and approved the final version of the manuscript.

Funding

This work was supported by Nanjing Chengshi (TheraRNA) Biomedical Technology Co. Ltd. and the Priority Academic Program Development of Jiangsu Higher Education Institutions (PAPD).

Declarations

Competing interests

The authors declare no competing interests.

Additional information

Supplementary Information The online version contains supplementary material available at https://doi.org/10.1038/s41598-025-21924-4.

Correspondence and requests for materials should be addressed to S.X., Q.M. or Y.Q.